

## Research Article

## Modeling and Predicting the Important Properties of the PVC/Glass Fiber Composite Laminates in the Production Process by the TLBO-ANFIS Approach

E. Sherkatghanad<sup>1</sup>, H. Moslemi Naeini<sup>1\*</sup>, A.H. Rabiee<sup>2</sup>, A. Zeinolabedin Beygi<sup>1</sup>, V. Zal<sup>1</sup> and L. Lang<sup>3</sup>

<sup>1</sup> Department of Mechanical Engineering, Tarbiat Modares University, Tehran, Iran

<sup>2</sup> Department of Mechanical Engineering, Arak University of Technology, Arak, Iran

<sup>3</sup> School of Mechanical Engineering and Automation, Beihang University, Beijing, China

## ARTICLE INFO

*Article history:*

Received 20 July 2021

Reviewed 21 September 2021

Revised 15 October 2021

Accepted 23 October 2021

*Keywords:*

Thermoplastic composites

ANFIS network

Teaching-learning-based

algorithm

Hot press

## ABSTRACT

In this paper, by considering the temperature, time, and process pressure, as the most important factors in producing the thermoplastic composites, an experimental design was performed. An adaptive neuro-fuzzy inference system (ANFIS) was utilized to estimate the important characteristics containing flexural strength, porosity volume ratio, fiber volume ratio, and flexural modulus. Then, the parameters of the ANFIS network were optimized by the teaching-learning-based optimization (TLBO) algorithm. For the purpose of modeling material behavior in the process, the experimental results were utilized for the training and validation of the adaptive inference system. The accuracy of the obtained model has been investigated by using different graphs, based on the statistical criteria of the mean absolute error, correlation coefficient, mean square error, and the percentage of mean absolute error. Based on the obtained results, the TLBO-ANFIS approach has been very effective in estimating the above-mentioned properties in the production process. The network error for estimating flexural strength, porosity volume ratio, fiber volume ratio, and flexural modulus in the training section was equal to 0.159%, 0.0003%, 1.074%, and 0.0001%, and the corresponding values were equal to 0.852%, 42.413%, 33.95%, and 4.894% in the testing section.

© Shiraz University, Shiraz, Iran, 2021

### 1. Introduction

Due to the great specific strength and stiffness of composite materials compared to other engineering materials like metals, many industries such as automobile, aerospace, and the military are focused on applying composite materials with the intention of producing lighter structures, mechanisms, and parts. Product weight plays a vital role in the success of their missions. It also reduces energy consumption, which has

a special place in the transportation industry [1]. Moreover, one of the challenges of using composite materials is the production method of the desired shape. Conventional forming processes are commonly used in a variety of products due to their high speed, excellent output, and low cost, but there are challenges to using these methods to make composite products [2]. Therefore, process investigation of composite forming is essential due to the intricate mechanical performance of composite materials, especially in different layers.

\* Corresponding author

E-mail address: [Moslemi@modares.ac.ir](mailto:Moslemi@modares.ac.ir) (A. Moslemi Naeini)

<https://doi.org/10.22099/IJMF.2021.41242.1190>

Composite materials with polymer matrices are allocated into two main clusters, each containing thermoset and thermoplastic matrices. Although the making and applying of thermoplastic-based composite materials are restricted due to the production complications and high production costs, many industries are more interested in these advanced materials because of their higher quality characterization, including impact strength, formability at high temperatures, environmental resistance, fracture toughness, recyclability, and indefinite storage life [3-5]. Since thermoplastic polymers' viscosity is usually greater than that of thermoset polymers, in most cases their wetting process is very complicated and impregnation is not satisfactory [6]. The impregnation of fiber and the quality of bonding will result in better reliability and more suitable mechanical properties. This will be achieved due to the fact that better impregnation creates higher mechanical characteristics in such advanced structural materials, and regulates the allowable force and the quality of stress arrangement in manufactured goods [7]. Many investigations with different methods have been carried out to develop the impregnation feature of thermoplastic composites. The PEEK/carbon fiber composites impregnation is investigated by Ye et al. [8] and the effects of different parameters of the production such as pressure, temperature, and time are studied on the mechanical characteristics of the specimen. Macro and micro impregnation in the glass and carbon fibers are studied by Mayer et al. [9] while liquefied thermoplastic nylon 6.6 is utilized in an unceasing production method. Han et al. [10] was able to improve the mechanical characteristics by improving the quality of impregnation of the investigated thermoplastic composites through sizing the fibers. Thermoplastic composite characteristics such as physical and mechanical ones of glass fibers with different sizes have been investigated by Ferreira et al. [11]. Jonoobi et al. [12] studied the mechanical characteristics and impregnation excellence of some bio-based/nanofiber thermoplastic composite materials. Zal et al. [13-16] investigated the field of the

main parameter effects on properties such as flexural strength and modulus of a thermoplastic-based laminated composites and investigated the failure mechanisms and impregnation quality. The most important factors in designing a composite structure are the materials selection and structural pattern. The material selection and the arrangement of reinforced fibers are often determined by mechanical properties. The process selection and structural concepts are dominated by a set of financial and operational concerns. So far, a lot of research has been done on the design of composites and the effects of different materials and different arrangements of reinforced fibers on the structure of composites have been investigated [17]. Maciel et al. [18] investigated the manufacturing of advanced composites including nano-engineered poly vinylidene fluoride (PVDF) with the fibers which were aligned and accidentally oriented fibers. Köbler et al. used mathematical methods to analyze short fiber reinforced composite parts with different arrangements [19].

By utilizing an artificial neural network (ANN), we can transfer existing knowledge and rules into the network structure that it is processing. ANN has a very high learning capability. This method is a very convenient choice, especially when integrated with a fuzzy logic system. By incorporating artificial neural networks and fuzzy systems, an efficient approach was developed to model different systems. Each of these methods can overcome the weakness of the other, which leads to an increase in the efficiency of the fuzzy-neuro system. In recent years, many researchers have used the ANFIS system to model different engineering processes [20-21]. Yaghoobi et al. [22] used the neural network method and the GA for optimization of the hydroforming process. Based on the simulation of neuro-fuzzy inference system results, they made a matching, and analyzed the impact of pressure on the maximum thinning of the critical areas of products. Dadgar Asl et al. [23] optimized the parameters of the flexible roll forming process according to the bending angle based on longitudinal bow and wrinkling by using the ANN-based

Genetic Algorithm.

In this paper, for the first time, an ANFIS network is utilized to model the effect of important parameters in the production process (i.e., temperature, time, and pressure) to predict the flexural modulus, flexural strength, void volume fraction and fiber volume fraction. So far, this method has not been used to study the behavior and predict the mentioned outputs in the production process. For this purpose, the results of experiments performed to train and test the fuzzy inference system have been used. In addition, to achieve the optimal structure of the ANFIS system, the teaching and learning optimization algorithm has been utilized.

## 2. Experimental Method

In this research, the efficacies of the production factors comprising pressure, temperature, and time on the final product features of laminated fiberglass/PVC composites were assessed using the experimental data of the paper by Zal et al. [13]. The applied production methods in the experiments such as stacking and hot pressing, which have been utilized to make the PVC/fiberglass composite laminates, were filmed, different patterns and orientations with  $[0/90]_{10}$  layups have been set, and finally the 3 mm products were exerted. According to the standard of ASTM D790, the basic mechanical characteristics of the specimens were assessed by applying a three-point bending test. Finally, using microscopic images, the impregnation quality has been evaluated. One of the most important aims of this paper is the investigation into predicting the impregnation quality of PVC/fiberglass composite materials as well as finding the appropriate processing factors condition. To achieve this goal, PVC/woven fiberglass composite materials have been manufactured. Then key production factors such as, temperature, pressure and time of the process have been altered and their effects on the main parameters including flexural modulus and strength of the specimens were examined. The quality of the impregnation and bonding in the middle of the fiber layer and matrix, as well as the specimen failure mechanisms were investigated. Safari

et al. [24] analyzed the effects of the main factors in the creep forming production method, including temperature and time, on the spring-back of shaped fiber metal laminate.

As mentioned, one of the most common tests to assess inner-laminar properties and the quality of the impregnation of the laminated composites is three-point bending [25-27]. Consequently, this technique was utilized in this study and repeated three times to assess the specimens. The outcomes of these tests demonstrate dissimilar deflection performance for the specimens because of the difference in bonding strength between the matrix and fibers as well as the impregnation quality. The outcomes in the diagram of load and displacement for several of the testers and the used three-point bending test setup are illustrated in Fig. 1 [13].

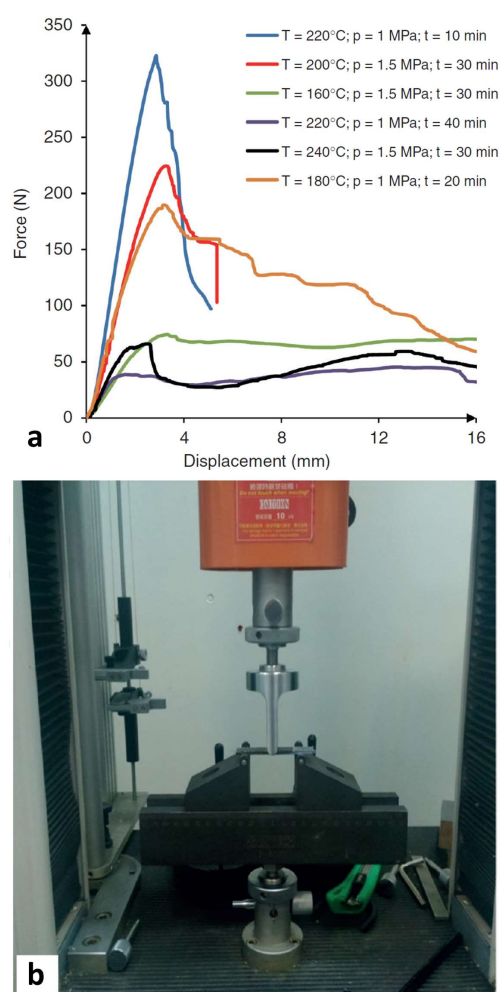
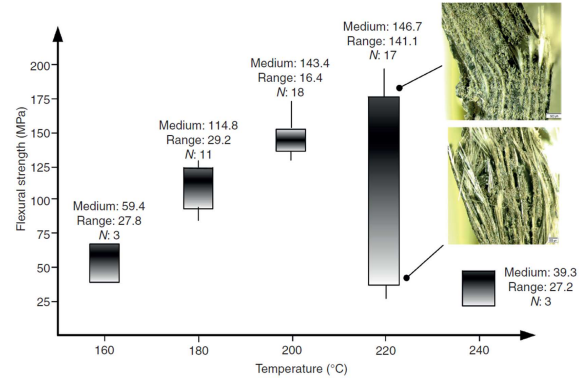


Fig. 1. (a) Load-displacement curves of several specimens, (b) the setup of three-point bending test [13].

As shown in Fig. 2, if the process temperatures are lower than 220°C, any rise in temperature will increase the flexural strength, but two other factors change the strength as well. For specimens manufactured at 220°C, the effect of production process time is extreme and any difference in the production time meaningfully changes the strength. The temperature effect on the specimens' flexural strength in different settings of the production process time and pressure is depicted in Fig. 2.

In Table 1 [13], the intended inputs are provided with the test results. The values of the output variables for each of the 18 experiments are given.

The difference in mechanical characteristics in the final specimens is mostly determined by the quality of impregnation and the diffusion of the matrix between fiber layers. To describe the parameters' effects on the mechanical features, as illustrated in Fig. 3, specimen's SEM pictures of diverse process settings are illustrated. As understood from Fig. 3(a), the matrix diffusion among yarns does not take place in the specimen which has a treating temperature of about 160°C; consequently, the materials have been stuck together as discrete films. While the PVC layers are softer near 160°C to bind to the fibers than to create a combined piece, the stickiness



**Fig. 2.** The effect of temperature in the production process on the flexural strength of the specimens (N, shows the total measured specimens, and range means outcomes deviation), the 200°C manufactured specimens have the minimum reliance on the other factors [13].

is not suitable enough to create a final uniform specimen. Consequently, the layers slip over each other through stacking because of weak connections between them. As it is shown in Fig. 3(b), small progress in the impregnation happened where the process temperature was 180°C; but the stickiness is still high, making all the fibers wet. Fig. 3(c) shows an SEM image where the process temperature was 200°C, where the PVC enters the fibers suitably. However, in the condition of 220°C and the timeframe of 10 min, the quality of impregnation

**Table 1.** Trials performed and response values for flexural strength and modulus, void volume fraction, volume fraction [13]

No.	Flexural modulus (GPa)	Flexural strength (MPa)	Void volume fraction (%)	Fiber volume fraction (%)	Density (kg/m <sup>3</sup> )	Processing pressure (MPa)	Processing time (min)	Processing temperature (°C)
1	8.4	153.6	5.2	27.7	1571	1	20	220
2	4.8	28.2	29.7	28.3	1257	1	40	220
3	9.4	136	1.9	26.9	1602	2.5	30	200
4	10.7	149	3.2	25.8	1573	1.5	30	200
5	10.8	151.1	2.3	26.6	1593	1.5	50	200
6	7.4	99.2	5.9	25.5	1533	2	20	180
7	3	54.2	8.8	24.2	1479	1.5	30	160
8	4.9	33.6	30.8	28.2	1251	2	40	220
9	8.3	145.8	4.4	25.5	1554	0.5	30	220
10	9.7	147.2	2	26.7	1598	2	20	220
11	8.7	120.4	3.6	25	1556	2	180	180
12	5.5	35.5	35.7	25.9	1158	1.5	240	240
13	10.1	138	3	26.4	1583	1.5	200	200
14	7.6	106.5	4.8	25.1	1542	1	180	180
15	7.1	110	3.7	25.9	1566	1	180	180
16	10.4	153.6	3	26.3	1581	1.5	200	200
17	9.7	170.7	1.2	28	1625	0.5	220	220
18	10.3	189	2.2	28.3	1617	2	220	220

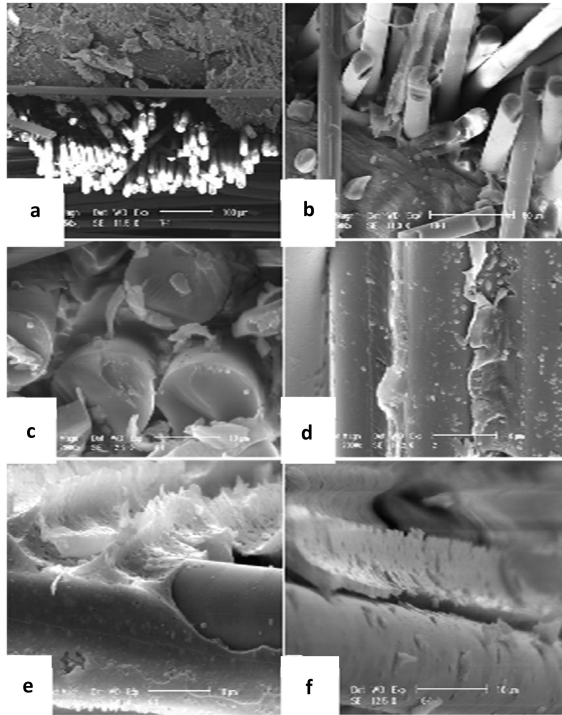


Fig. 3. SEM images of fiber/matrix impregnation of the composite layers shaped at changed settings [13].

was superior, and the matrix bordered all the fibers entirely (Fig. 3(d)); this shows the suitable decrease of PVC matrix stickiness at 220°C can be used to make the fibers wet. Though 220°C seems to be the appropriate temperature to reach an excellent impregnation, more increase in the time or temperature of the process makes an intense decrease in the mechanical features. By enhancing the time of the process, the PVC matrix was slowly ruined making the bonding weaker. Fig. 3(e) and 3(f) illustrate SEM images of the ruined specimens.

### 3. Optimized Intelligent Modeling

#### 3.1. ANFIS

The adaptive neuro-fuzzy inference system (ANFIS) has the advantages of both linguistic and numerical methods. The ANFIS network is trained without the need for expert knowledge while this is essential for the fuzzy logic system. ANFIS utilizes the ability of artificial neural networks to detect patterns and categorize data. The ANFIS has less memory error compared to the artificial neural network and has a clearer architecture for the user. Other advantages of the

ANFIS system include nonlinear capability, fast learning and adaptability. Similar to fuzzy logic systems, the structure of ANFIS contains two sections: the antecedent and subsequent. These two sections are merged with each other by a set of rules. ANFIS is known as a multilayer network that has five distinct layers. Takagi-Sugeno (TS) fuzzy system is a variation of such systems that includes multiple inputs and only one single output, as presented in Fig. 4. This system consists of two inputs  $x$  and  $y$ , and an output  $f$ , which are merged by the rules as:

**Rule 1:** If ( $x$  equals  $A_1$ ) and ( $y$  equals  $B_1$ ), then  $f_1 = p_1x + q_1y + r_1$

**Rule 2:** If ( $x$  equals  $A_2$ ) and ( $y$  equals  $B_2$ ), then  $f_2 = p_2x + q_2y + r_2$

In this system,  $A_i$  and  $B_i$  are the fuzzy sets, and  $f_i$  is the output set. Furthermore,  $p_i$ ,  $q_i$ , and  $r_i$  are designing constants that are obtained during the learning procedure. In particular, the computations in each layer are explained below; if the output of each is defined as  $O_i^j$  where  $i$  and  $j$  are indexes of node and layer, respectively.

**Layer 1:** In the first layer, each node is equal to a fuzzy layer where the output is related to the membership function (MF) degree. The constants of each node determine the shape of the corresponding membership function. If we utilize Gaussian membership functions, we have:

$$\mu_{Ai}(x) = e^{-\frac{1}{2}\left(\frac{x-c_i}{\sigma_i}\right)^2}, \quad i = 1, 2 \quad (1)$$

in which,  $x$  is the node input and  $c_i$ ,  $\sigma_i$  the center and width of the Gaussian membership, respectively.

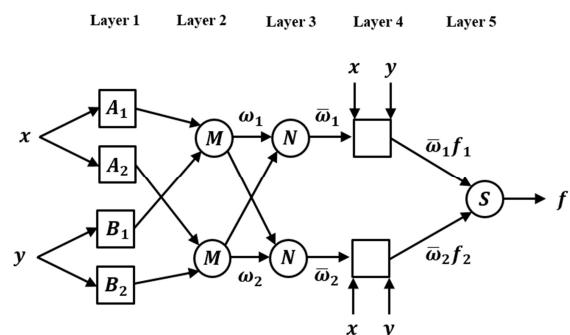


Fig. 4. ANFIS network structure.



**Layer 2:** In the second layer, the inputs of each node are reproduced together, and the rule firing strength is computed as:

$$O_i^2 = \omega_i = \mu_{A_i}(x)\mu_{B_i}(y), \quad i = 1, 2 \quad (2)$$

in which,  $\mu_{A_i}$  is the degree of MF of  $x$  in the fuzzy set  $A_i$ ,  $\mu_{B_i}$  is the degree of MF of  $y$  in the fuzzy set  $B_i$ .

**Layer 3:** The nodes in third layer calculate the comparative weight of the rules, where  $\omega_i^n$  is the normalized fire intensity of rule  $i$ .

$$O_i^3 = \omega_i^n = \frac{\omega_i}{\omega_1 + \omega_2}, \quad i = 1, 2 \quad (3)$$

**Layer 4:** This layer is recognized as the rule layer, which is attained by producing the rule firing strength by the output of the Takagi-Sugeno fuzzy inference model.

$$O_i^4 = \omega_i^n f_i = \omega_i^n (p_i x + q_i y + r_i), \quad i = 1, 2 \quad (4)$$

**Layer 5:** The final layer included is an individual node in which all the inputs are merged with each other:

$$O_i^5 = \sum_{i=1}^2 \omega_i^n f_i = \frac{\omega_1 f_1 + \omega_2 f_2}{\omega_1 + \omega_2}, \quad i = 1, 2 \quad (5)$$

For a better and simpler understanding, the ANFIS formulation presented in this section (Eqs. (1) to (5)) is a basic example of an ANFIS network with two inputs, each with two fuzzy sets. For this reason,  $i = 1, 2$  is used in the relations. Obviously, by increasing inputs as well as increasing fuzzy sets, the values of  $i$  increase to the number of fuzzy sets.

According to the description given, it is clear that the first and fourth layers are adaptive layers in which  $\sigma_i$  and  $c_i$  are adaptive parameters. In the fourth layer,  $r_i$ ,  $q_i$ , and  $p_i$  are also other adaptive parameters known as output parameters. Numerous optimization algorithms have been utilized to improve the accuracy of the ANFIS model. The teaching-learning-based optimization algorithm is one of the most effective optimization approaches used to find the optimal parameters of the ANFIS network in this study.

### 3.2. TLBO

The teaching-learning-based optimization method which is designed on the foundation of the effect that a teacher has on students has two parts: teaching and learning phases. In a classroom, a teacher is a person who has the best knowledge and can teach the subject to students very well.

**Teaching section:** In this section, the teacher is selected from among the students based on his or her high knowledge. The teacher tries to raise the average of the class based on the information he or she has, although none of the students can reach his level, but instead they reach the new average. As a result, a new population with a new average of  $M_2$  is created with the presence of a teacher ( $T_2$ ). The process of improving the average of the classroom continues until they achieve an optimal score in the teaching phase. This process is illustrated in Fig. 5(a). The mathematical equations of the first phase are as follows:

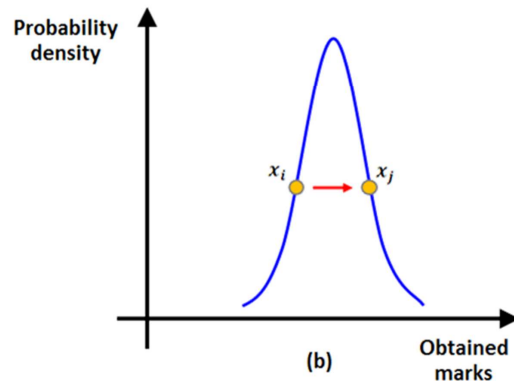
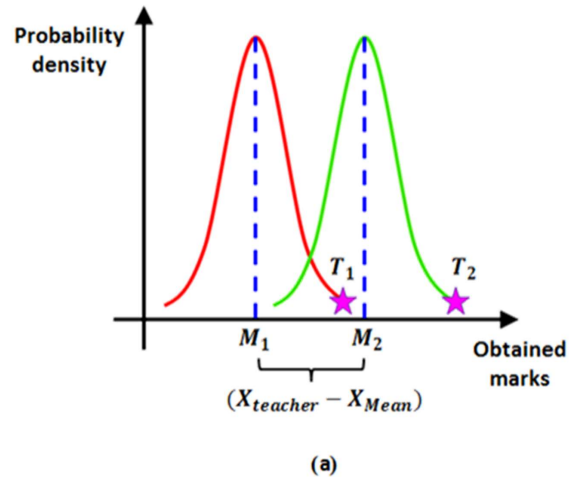


Fig. 5. (a) Teacher phase, and (b) learner phase.

$$X_{new} = X_{old} + r(X_{teacher} - T_f \times Mean) \quad (6)$$

in which,  $r$  is a random vector that determines the success rate of a student in the teaching process and is considered between zero and one. Furthermore,  $T_f$  indicates the teacher success rate with values  $\{2,1\}$ .

**Learning section:** In this phase, students learn from each other, which results in the process of improving the level of the students. According to Fig. 5(b), two students are randomly selected, among which, the first one learns from the second. Here, depending on the score of these selected students, two situations arise:

Case 1: If the  $X_i$  score is worse than  $X_j$  but, a poor student ( $X_i$ ) requests to learn from a student with better grades ( $X_j$ ). The mathematical relation will be as follows:

$$X_{i,new} = X_i + r(X_j - X_i) \quad (7)$$

in which  $r$  is a random vector that determines the success rate of a student in the learning process and is between zero and one.

Second case: if  $X_i$  scores are better than  $X_j$  the same situation as the latter arises, except that  $X_j$  learns from  $X_i$  and its mathematical relation is as follows:

$$X_{i,new} = X_i + r(X_i - X_j) \quad (8)$$

It is important to know that in both the teacher and the learner phases, the value of the target function is

computed by obtaining the new  $X_{i,new}$ ; and if this score is higher than the score of the old version of the target function, the student information will be updated. Otherwise, the previous information will remain unchanged.

#### 4. Results and Discussion

In this study, 18 numbers of experimental data for testing the system, which includes three inputs of pressure, time and temperature process, and four outputs of flexural strength and modulus, fiber volume ratio, and void volume ratio were obtained. This data is separated into two subsets, 70% for teaching, and 30% for testing of ANFIS. Errors in experimental data are unavoidable, although these errors are larger in some tests. If these tests are placed in the training section, it will lead to improper network training, and if located in the test section, it will cause a high network error in this section. The best way to separate the tests into two training and test sections, is random selection, which is done by software code. In this case, there is no intentional intervention in the data separation by the user. The parameters of the input and output MFs, as well as the fuzzy rules, are optimized by the teaching-learning optimization algorithm. Figs. 6-9 display the optimized Gaussian MFs for flexural strength and modulus, fiber volume ratio, void volume ratio outputs.

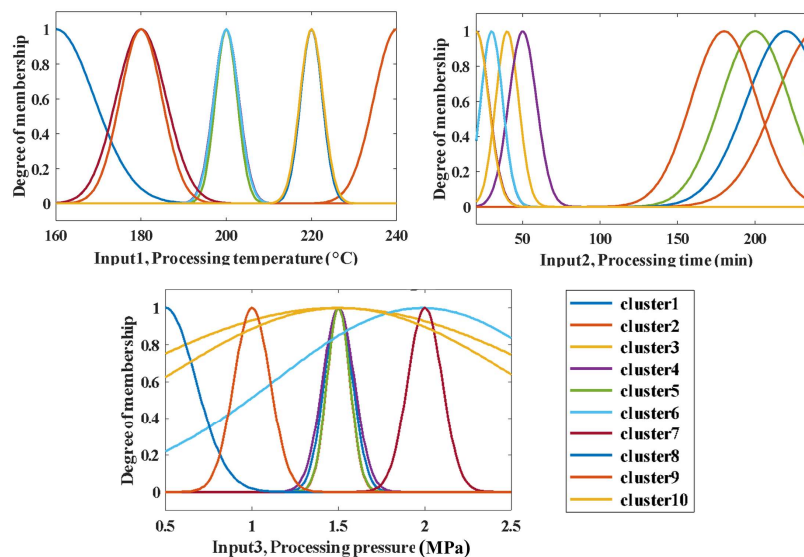


Fig. 6. Optimized MFs for temperature, time, and process pressure inputs for fiber volume fraction.

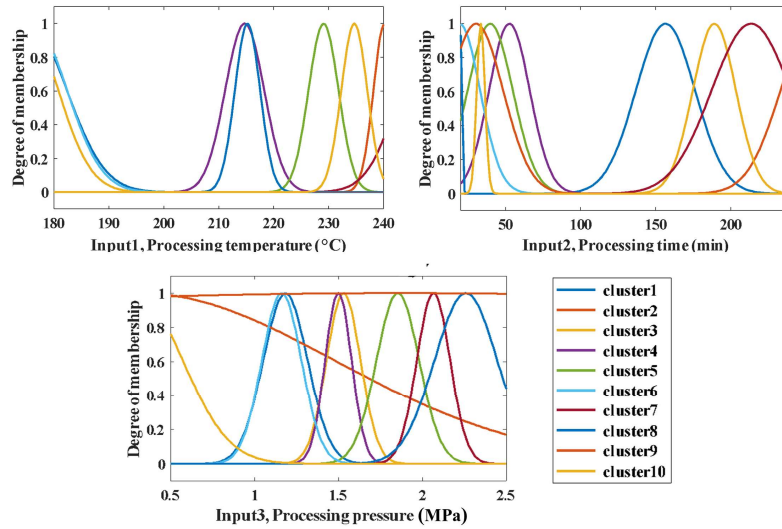


Fig. 7. Optimized MFs for temperature, time, and process pressure inputs for void volume fraction.

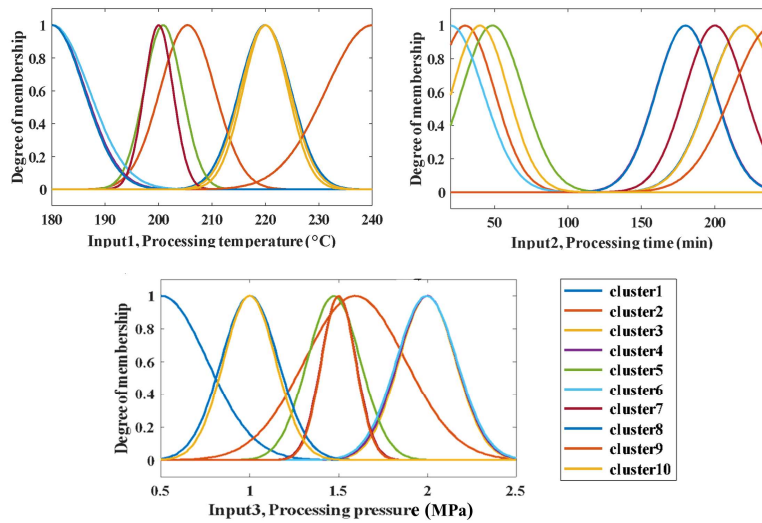


Fig. 8. Optimized MFs for temperature, time, and process pressure inputs for flexural strength.

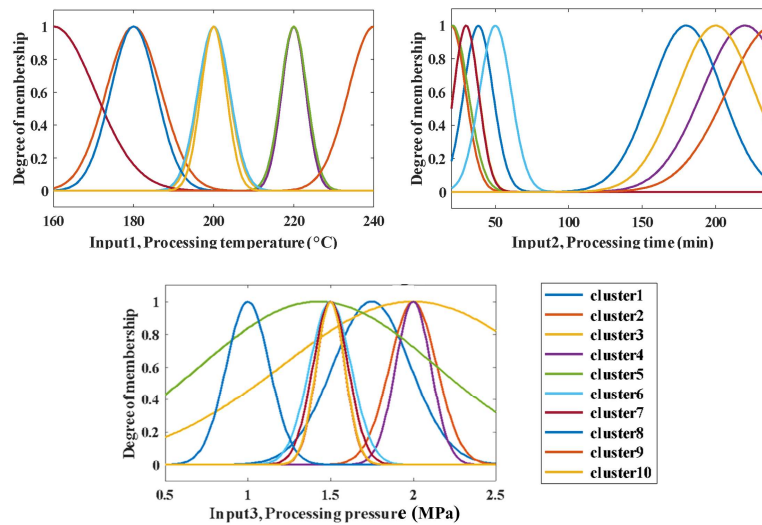


Fig. 9. Optimized MFs for temperature, time, and process pressure inputs for flexural modulus.



Here are some graphical methods utilized to measure the efficiency of the proposed model. Fig. 10 displays the approximated data by the ANFIS model alongside

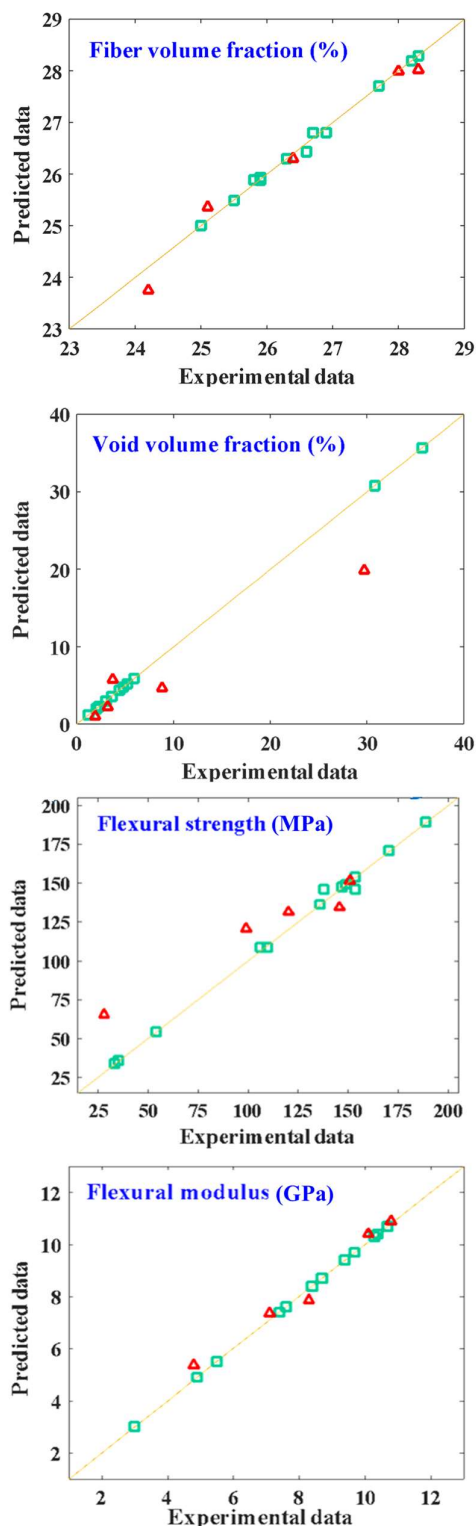


Fig. 10. Comparison between experimental data and prediction data.

with actual data for each of the outputs of the production process. In these diagrams, the square symbols are related to the data utilized in the teaching section, and the triangular symbols are related to the data of the ANFIS testing section. The middle  $y = x$  is also a reference to determine the accuracy of the model. As it is seen, the correctness of the network is very high for predicting the data of the teaching phase for all outputs. It can also be seen that the network accuracy for estimating the outputs of flexural strength and modulus, fiber volume ratio, void volume ratio is also high. On the other hand, the estimated data for void volume fraction and flexural strength outputs are farther from the centerline, which indicates a larger network error in predicting these outputs. Furthermore, Fig. 11 shows the values of void volume fraction, fiber volume fraction, flexural modulus and flexural strength of the production process for real and predicted data in both teaching and testing phases. In these diagrams, the purple and orange lines represent the practical data for the teaching and testing sections. The square and triangular symbols indicate the data estimated by the ANFIS model related to the teaching and testing phases, respectively. As can be seen in these diagrams, the ANFIS network is coincident with the data of the teaching section for all outputs (the square symbols correspond to the purple lines). It is also clear from the second part of the diagrams (orange section) that the network has been able to predict the data related to the testing section very well; however, the estimation accuracy for the fiber volume fraction and flexural modulus is higher than that of the void volume fraction and flexural strength. Furthermore, Fig. 12 shows the percentage of mean absolute error related to the teaching and testing sections for modeling void volume fraction, fiber volume fraction, flexural modulus and flexural strength. In this figure, the teaching section is shown with a green background color, and the testing section is shown with a yellow background color. Based on the figures, the error values for all outputs are lower in the teaching section than in the testing section. Moreover, a higher error in predicting the output of void volume fraction and flexural strength in the test section is well observed.

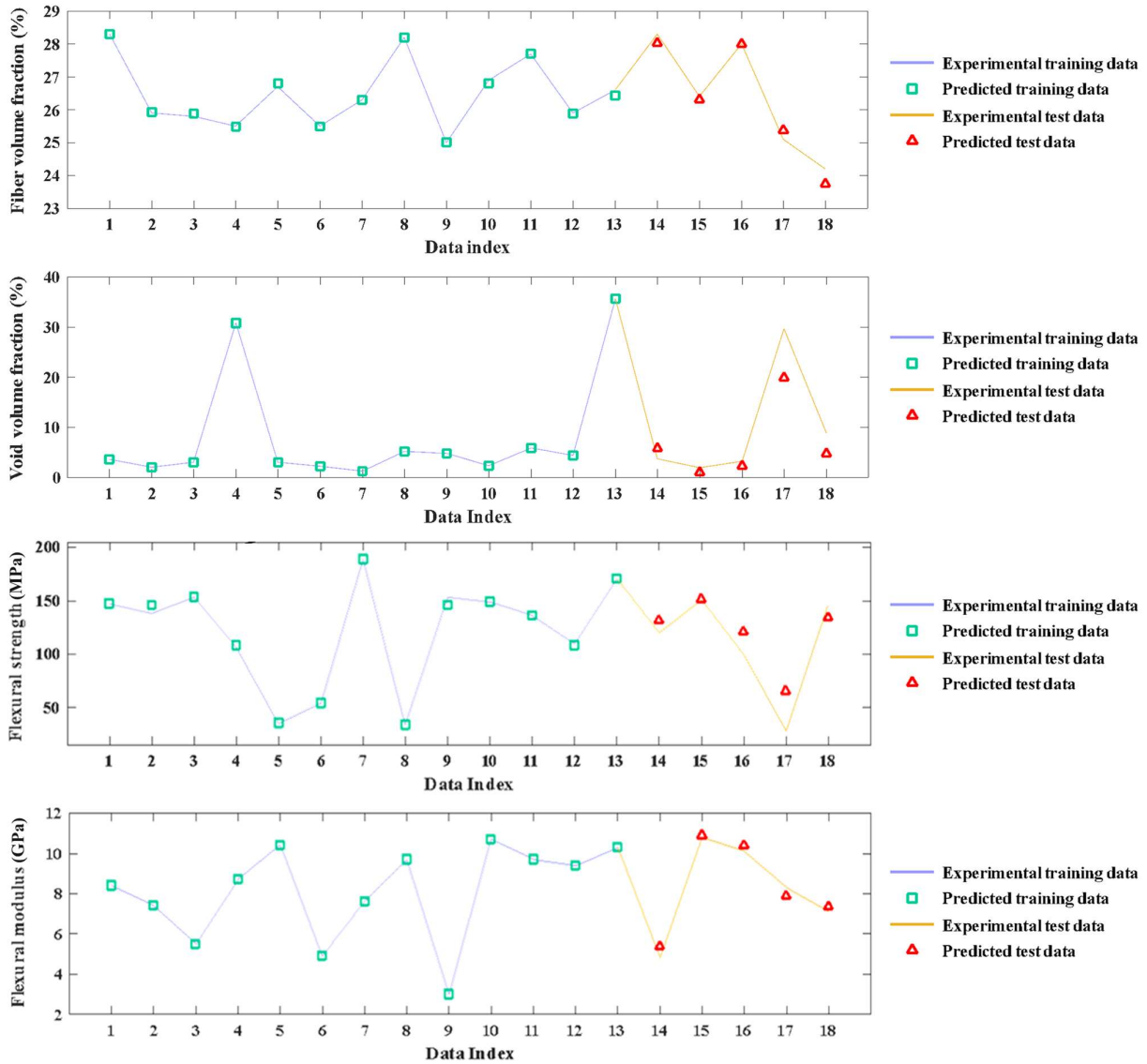


Fig. 11. Differences between experimental data and test data for predicting outputs.

In order to quantitatively measure the accurateness of the attained ANFIS network, the criteria of root mean square error, mean absolute error, correlation coefficient, and percentage of the mean absolute error have been used. How to calculate these criteria is presented in Eqs. (9)-(12), respectively.

$$RMSE = \sqrt{\frac{1}{n} \times \sum_{i=1}^n (O_A - O_P)^2} \quad (9)$$

$$MAE = \frac{1}{n} \sum_{i=1}^n |O_A - O_P| \quad (10)$$

$$R = \frac{\sum_{i=1}^n [(O_A - \bar{O}_A)(O_P - \bar{O}_P)]}{\sqrt{[\sum_{i=1}^n (O_A - \bar{O}_A)^2][\sum_{i=1}^n (O_P - \bar{O}_P)^2]}} \quad (11)$$

$$MAPE = \frac{100\%}{n} \sum_{i=1}^n \left| \frac{O_A - O_P}{O_A} \right| \quad (12)$$

In these relations,  $O_A$  is the value of output measured for sample  $i$ , and  $O_P$  is the output predicted for sample  $i$ ,  $\bar{O}_A$  is the mean of the measured data, and  $\bar{O}_P$  is the mean of the estimated data. To check the correctness of the model, the above-mentioned criteria are calculated for the teaching and testing phases which are listed in Table 2.

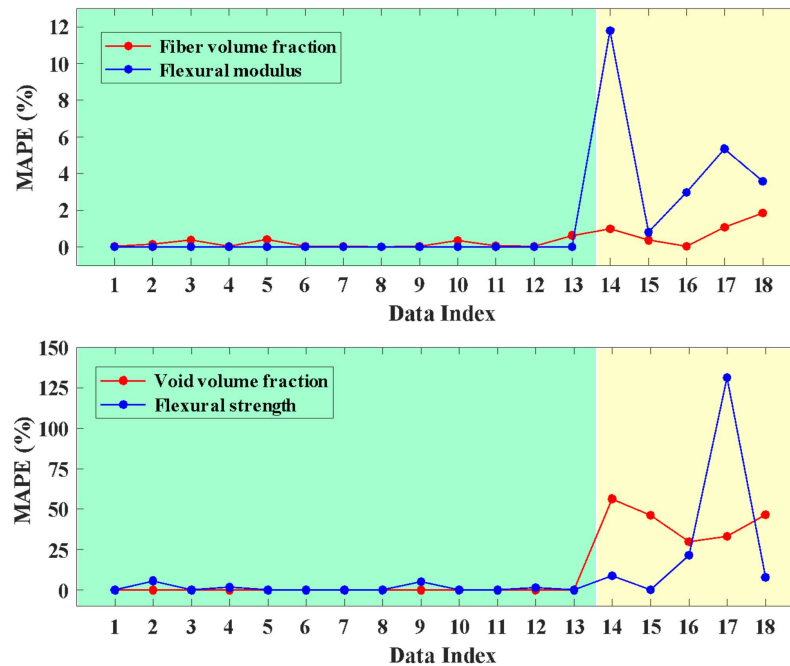


Fig. 12. Error of experimental data and test data for fiber volume fraction, void volume fraction, flexural strength and flexural modulus approximation.

From the values presented in Table 2, it can be understood that the obtained model has generally been effective in predicting all outputs of the production process, although the accuracy in estimating fiber volume fraction and flexural modulus was higher. The RMSE and MAE criteria are very small, especially for the teaching section. These criteria are not enough for evaluating the model. In the following, MAPE and R criteria are used to determine the value of error relative to the values of the data. The correlation coefficient R for the teaching section is very high (close to one), which indicates the complete coincidence of the experimental data with the predicted data in the teaching section. The correlation coefficient for the test

section is also very high for all outputs ( $R > 0.97$ ), which specifies the high accuracy of the obtained system.

In addition, the MAPE error in the testing section is higher than the one obtained from the teaching section. This is quite normal because in the teaching section all training data is used. However, the evaluation of the system is founded on test data and this data has not been utilized in the network teaching part. As a result, due to the errors in the practical results, this amount of error can be expected. Moreover, the higher error in predicting void volume fraction and flexural strength indicates the higher accuracy of the ANFIS model in predicting fiber volume fraction and flexural modulus.

Table 2. The RMSE, MAE, R and MAE criteria for modeling fiber volume fraction, void volume fraction, flexural strength and flexural modulus

		RMSE	MAE	R	MAPE (%)
Fiber volume fraction	Train	0.066493	0.042317	0.997844	0.159903
	Test	0.26672	0.217867	0.988865	0.852331
Void volume fraction	Train	0.000125	4.44E-05	1	0.000389
	Test	4.894411	3.572525	0.975539	42.41306
Flexural strength	Train	3.135467	1.469346	0.997933	1.074266
	Test	20.38059	16.16196	0.979542	33.95702
Flexural modulus	Train	1.75E-05	1.22E-05	1	0.000181
	Test	0.368455	0.329811	0.988639	4.89478

## 5. Conclusion

In this study, the ANFIS network optimized by TLBO algorithm is used to model the production process based on the input variables (pressure, time and temperature) and output variables (void volume fraction, fiber volume fraction, flexural modulus and flexural strength). The analysis of the results displays that the obtained ANFIS structure is very effective for the present procedure, and by using this model the values considered outputs can be calculated based on the changes of the input variables. The correlation coefficient for modeling the output variables in the teaching and testing sections are close to one, which indicates a very good agreement between the results estimated by the ANFIS and the experimental data. It can also be seen that the network error for estimating fiber volume fraction, void volume fraction, flexural strength, and flexural modulus in the teaching section is equal to 0.159%, 0.0003%, 1.074%, and 0.0001%, and the corresponding values are equal to 0.852%, 42.413%, 33.95%, and 4.894% in the testing section.

## 6. References

- [1] Q. Liu, Y. Lin, G. Sun, Q. Li, Lightweight design of carbon twill weave fabric composite body structure for electric vehicle, *Composite Structures*, 97 (2013) 231-238.
- [2] S. Davey, R. Das, W.J. Cantwell, S. Kalyanasundaram, Forming studies of carbon fibre composite sheets in dome forming processes, *Composite Structures*, 97 (2013) 310-316.
- [3] S.F. Hwang, K. Hwang, Stamp forming of locally heated thermoplastic composites, *Composites Part A: Applied Science and Manufacturing*, 33(5) (2002) 669-676.
- [4] W. Hufenbach, R. Böhm, M. Thieme, A. Winkler, E. Mäder, J. Rausch, M. Schade, Polypropylene/glass fibre 3D-textile reinforced composites for automotive applications, *Materials & Design*, 32(3) (2011) 1468-1476.
- [5] W. Wu, L. Xie, B. Jiang, G. Ziegmann, Simultaneous binding and toughening concept for textile reinforced pCBT composites: Manufacturing and flexural properties, *Composite Structures*, 105 (2013) 279-287.
- [6] H. Parton, I. Verpoest, In situ polymerization of thermoplastic composites based on cyclic oligomers, *Polymer composites*, 26(1) (2005) 60-65.
- [7] J.L. Thomason, U. Nagel, L. Yang, D. Bryce, A study of the thermal degradation of glass fibre sizings at composite processing temperatures, *Composites Part A: Applied Science and Manufacturing*, 121 (2019) 56-63.
- [8] L. Ye, K. Friedrich, J. Kästel, Y.W. Mai, Consolidation of unidirectional CF/PEEK composites from commingled yarn prepreg, *Composites science and technology*, 54(4) (1995) 349-358.
- [9] C. Mayer, X. Wang, M. Neitzel, Macro-and micro-impregnation phenomena in continuous manufacturing of fabric reinforced thermoplastic composites, *Composites Part A: Applied Science and Manufacturing*, 29(7) (1998) 783-93.
- [10] S.H. Han, H.J. Oh, S.S. Kim, Evaluation of the impregnation characteristics of carbon fiber-reinforced composites using dissolved polypropylene, *Composites science and technology*, 91(2014) 55-62.
- [11] N. Ferreira, C. Capela, J.M. Ferreira, J.M. Costa, Effect of water and fiber length on the mechanical properties of polypropylene matrix composites, *Fibers and Polymers*, 15(5) (2014) 1017-1022.
- [12] M. Jonoobi, Y. Aitomäki, A.P. Mathew, K. Oksman, Thermoplastic polymer impregnation of cellulose nanofibre networks: morphology, mechanical and optical properties, *Composites Part A: Applied Science and Manufacturing*, 58 (2014) 30-35.
- [13] V. Zal, H. Moslemi Naeini, A.R. Bahramian, A.H. Behraves, B. Abbaszadeh, Investigation and analysis of glass fabric/PVC composite laminates processing parameters, *Science and Engineering of Composite Materials*, 25(3) (2018) 529-540.
- [14] V. Zal, H. Moslemi Naeini, A.R. Bahramian, B. Abbaszadeh, Experimental evaluation of blanking and piercing of PVC based composite and hybrid laminates, *Advances in Manufacturing*, 4(3) (2016) 248-256.
- [15] V. Zal, H. Moslemi Naeini, A.R. Bahramian, J. Sinke, Investigation of the effect of temperature and layup on the press forming of polyvinyl chloride-based composite laminates and fiber metal laminates, *The International Journal of Advanced Manufacturing Technology*, 89(1-4) (2017) 207-217.
- [16] V. Zal, H. Moslemi Naeini, A.R. Bahramian, H. Abdollahi, A.H. Behraves, Investigation of the effect of processing temperature on the elastic and viscoelastic properties of PVC/fiberglass composite laminates, *Modares Mechanical Engineering*, 15(11) (2016) 9-16.
- [17] K.J. Narayana, R.G. Burela, A review of recent research on multifunctional composite materials and structures

- with their applications, *Materials Today: Proceedings*, 5(2) (2018) 5580-5590.
- [18] M.M. Maciel, S. Ribeiro, C. Ribeiro, A. Francesko, A. Maceiras, J.L. Vilas, S. Lanceros-Méndez, Relation between fiber orientation and mechanical properties of nano-engineered poly (vinylidene fluoride) electrospun composite fiber mats, *Composites Part B: Engineering*, 139 (2018) 146-54.
- [19] J.Köbler, M.Schneider, F.Ospald, H.Andrä, R.Müller, Fiber orientation interpolation for the multiscale analysis of short fiber reinforced composite parts. *Computational Mechanics*. (2018) 61(6):729-50.
- [20] I. Maher, M.E.H. Eltaib, A.A. Sarhan, R.M. El-Zahry, Investigation of the effect of machining parameters on the surface quality of machined brass (60/40) in CNC end milling—ANFIS modeling, *The International Journal of Advanced Manufacturing Technology*, 74(1-4) (2014) 531-537.
- [21] M. Safari, V. Tahmasbi A.H. Rabiee, Investigation into the automatic drilling of cortical bones using ANFIS-PSO and sensitivity analysis, *Neural Computing and Applications*, (2021) 1-19.
- [22] A. Yaghoobi, M. Bakhshi-Jooybari, A. Gorji, H. Baseri, Application of adaptive neuro fuzzy inference system and genetic algorithm for pressure path optimization in sheet hydroforming process, *The International Journal of Advanced Manufacturing Technology*, 86(9) (2016) 2667-2677.
- [23] Y.D. Asl, Y.Y. Woo, Y. Kim Y.H. Moon, Non-sorting multi-objective optimization of flexible roll forming using artificial neural networks, *The International Journal of Advanced Manufacturing Technology*, 107(5) (2020) 2875-2888.
- [24] M. Safari, M. Salamat-Talab, A. Abdollahzadeh, A. Akhavan-Safar, L.F.M. da Silva, Experimental investigation, statistical modeling and multi-objective optimization of creep age forming of fiber metal laminates. *Proceedings of the Institution of Mechanical Engineers, Part L: Journal of Materials: Design and Applications*, 234(11) (2020) 1389-1398.
- [25] M. Valente, F. Sarasini, F. Marra, J. Tirillò, G. Pulci, Hybrid recycled glass fiber/wood flour thermoplastic composites: Manufacturing and mechanical characterization, *Composites Part A: Applied Science and Manufacturing*, 42(6) (2011) 649-657.
- [26] R. Yahaya, S.M. Sapuan, M. Jawaid, Z. Leman, E.S. Zainudin, Effect of layering sequence and chemical treatment on the mechanical properties of woven kenaf–aramid hybrid laminated composites, *Materials & Design*, 67 (2015) 173-179.
- [27] J.A.M. Ferreira, C. Capela, J.D. Costa, A study of the mechanical behaviour on fibre reinforced hollow microspheres hybrid composites, *Composites Part A: Applied Science and Manufacturing*, 41(3) (2010) 345-352.